Proceedings of ERAD 2006

Analysis of the radar distance error structure through a simulation approach

Xavier Llort[1], Marc Berenguer[1,2], Rafael Sánchez-Diezma[1], Daniel Sempere-Torres[1]

[1] Grup de Recerca Aplicada en Hidrometeorologia, Universitat Politècnica de Catalunya, Barcelona (Spain).

[2] McGill University, Montréal (Canada).

1 Introduction

Radar precipitation estimates are affected by inherent errors of different sources. Although sophisticated algorithms have been developed to correct several errors, final precipitation products are not free of errors. The study of the remaining errors affecting radar rainfall estimates is becoming as important as the retrieval estimates themselves.

One of the ways to express the uncertainty in radar products is through the use of ensembles (see, for example, Germann et al., 2006). In this probabilistic approach, the radar precipitation estimates are perturbed adding noise fields with given distribution and structure. To properly generate these ensembles a complete characterization of the error structure is necessary.

In this new role for the radar data uncertainty we propose a physical simulation approach to study the characteristics of errors affecting the radar measurements independently (see for example Bellon et al., 2005, Lee et al., 2005).

Three independent steps compose the proposed simulation framework: (1) the generation of 3D high-resolution precipitation fields; (2) the physical simulation of how a radar would observe these reference fields; (3) characterization of the errors.

Since it is well known that the uncertainty in radar estimates increases with the range, this error has been studied under this framework to do a step in its characterization and show the feasibility of this approach.

Section 2 summarizes the simulation framework proposed to characterize the different radar errors in this study. In Section 3 we propose an application example of this framework and in Section 4 the first results of this application are presented. Finally, Section 5 provides some preliminary conclusions.

Correspondence to: Xavier Llort.

llort@grahi.upc.edu

2 Simulation framework

This section briefly introduces the simulation framework proposed to characterize the different radar errors. It is based on three independent steps, each one described below.

2.1 Generation of reference fields

In a first step, we generate 3D high-resolution precipitation fields. These fields will be considered as the reference for the rest of the study.

To generate these reference fields, we use rainfall information measured close to the radar as starting point of a downscaling technique. The used downscaling technique (described in Llort et al., 2006) is based on a combination of a wavelet scale-analysis, Fourier spectral analysis and homotopic techniques.

In this technique, the first radar tilt is downscaled by a 2D wavelet model using a given Haar-base scale analysis. Once the first radar PPI is downscaled up to the requested resolution, the remaining tilts are downscaled by a homotopy of the observed VPR in order to preserve the vertical structure measured by the radar. In a last step, the polar dense values are transformed to a Cartesian grid using the "nearest neighbour" algorithm.

2.2 Simulation of radar observations

The second step of this framework is the simulation of radar observation of a given reference field located at a certain distance. To calculate this degraded field, we perform the convolution between the radar equation and the 3D precipitation field. The radar equation (e.g. Doviak and

Zrnic, 1992) relates the power received by the antenna and the target reflectivity, and can be expressed as:

$$\overline{P}(r_0) = \frac{P_t g^2 \lambda^2}{L^2(r_0)(4\pi)^3} \int_{Vres} \frac{|W_s|^2 f^4 \sigma}{r^4} dV \qquad (1)$$

The range weighting function ($|W_s|^2$) used in this study is the proposed in Doviak and Zrnic (1992), and the normalized power (f^4) is approximated by a Gaussian function:

$$f^4(\phi) = \exp\left(-\frac{8Ln(2)\phi^2}{\phi_3^2}\right) \qquad (2)$$

Where ϕ_3 is the 3dB power angle.

For each bin, the contribution of all reference field pixels to the total power has been calculated, and later on, we calculated the convolution between these weights and the corresponding values of the reference field to obtain the simulated field. This two-step process allows us to reduce computational time if several simulations with the same parameters are done over different reference fields (which is the case of the present work).

2.3 Analysis of the error structure

Once we have the reference fields and the radar-simulated fields, we can study the differences (the radar errors, if we consider the reference fields as "the truth").

This approach allows us to study the error separately, extracting for each one its characteristics (distribution, mean, variance, spatial and temporal correlation, etc.).

3 Application

As example of the described scheme, and in order to show its feasibility, we characterize radar errors induced by the distance.

The data used for this work is a set of 291 rainy volume scans measured with the C-band radar of the Spanish Institute of Meteorology (located in Corbera de Llobregat, close to Barcelona) between 12th October 2005 - 00:00 UTC and 16th October 2005 - 23:50 UTC. This event contains a mix of rainfall types, but stratiform images, showing a low bright band, are predominant.

Rainfall fields located into an area of 20 x 20 x 10 km^3, located close to the radar and over the sea, has been downscaled using the technique described above. Previous to the downscaling, the data has been corrected for the principal radar errors. We performed three iterations of the wavelet technique using a scale-law based on 100 rainy images (containing a mix of rainfall types). The final resolution for the Cartesian field has been set to 250 m in the three dimensions.

Observations of a radar located at several ranges between 15 and 140 km (see Fig. 1) have been simulated.

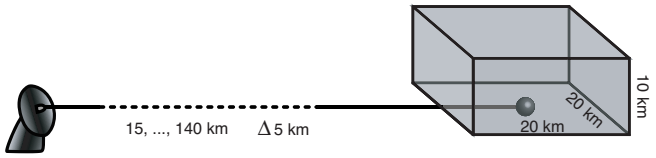

Fig. 1. Simulation scheme.

It is worth noting that the errors induced by the simulations are only due to beam broadening and the height increasing with range.

4 First results

In a first instance we calculated the correlation between the simulated fields and reference fields. Fig. 2 depicts the evolution with the distance of this parameter, and clearly shows how it decreases with distance.

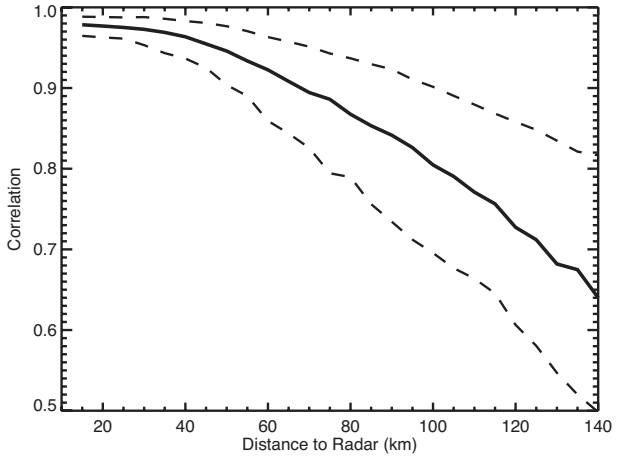

Fig. 2. Correlation between simulated and reference fields as a function of range. Solid line corresponds to the median of the 291 fields, and dashed lines correspond to the 25 and 75 percentiles.

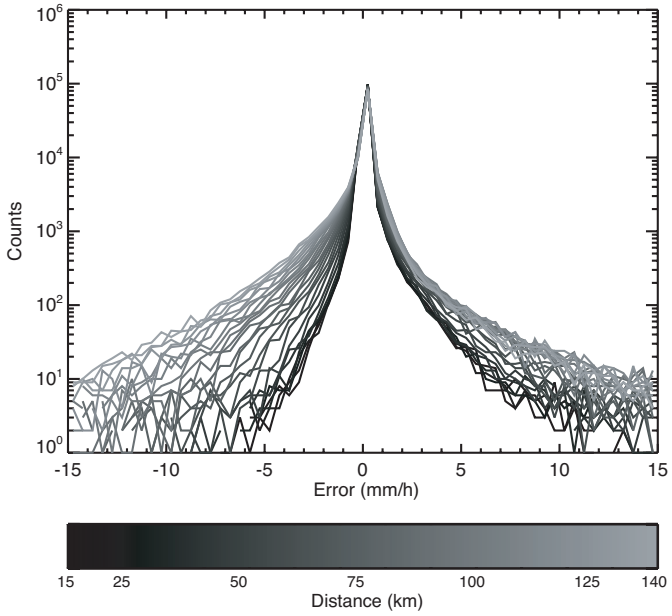

Fig. 3. Evolution with distance of the error fields pdf.

Some statistics of the error fields (i.e. difference between reference and simulated fields), have been calculated: pdf, mean, standard deviation and spatial correlation. Fig. 3 shows how the error distribution changes with the distance. In this figure it can be seen that the error distribution is similar for all the distances (Gaussian, but slightly skewed to the positive side) but becoming wider with the distance.

The variation of the error field mean (bias of the simulations) with distance is presented in Fig. 4. This figure shows how the radar overestimates the reference field up to a certain resolution from which the bias becomes close to zero. This phenomenon (enhanced in the accumulated fields; see Fig. 7) can be explained by the height of the bright band (relatively low), which was intercepted at close ranges. At farther ranges, the beam is over the bright band and the radar underestimates the reference fields. This effect should be further investigated using rain type classification in a future work.

Fig. 5 shows the standard deviation of the error fields as function of range. As it was expected, it increases with the distance.

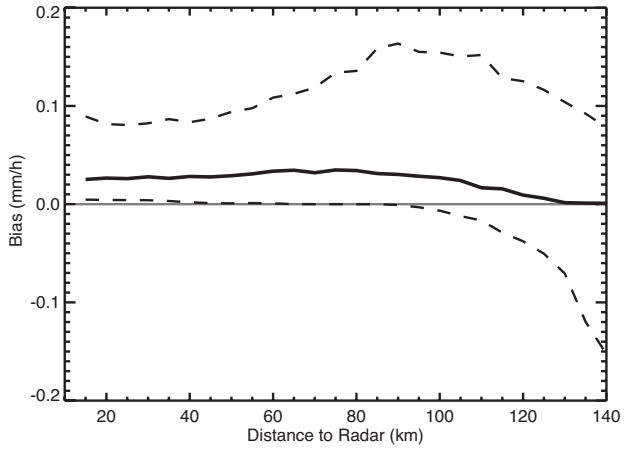

Fig. 4. Dependence of the bias with distance, that is, mean of the error fields. Solid line corresponds to the median of the 291 fields, and dashed lines to the 25 and 75 percentiles.

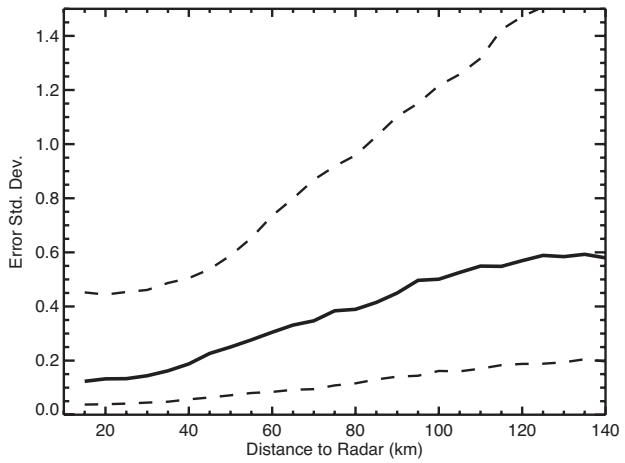

Fig. 5. Standard deviation of the error fields, as a function of range. Solid line corresponds to the median of the 291 fields, and dashed lines to the 25 and 75 percentiles.

In order to study the spatial correlation of the error fields, we calculate the Fourier power spectrum and we assume that can be fitted to a power-law:

$$\Gamma(f) \propto f^{-\beta} \tag{3}$$

Fig. 6 shows the dependence of the parameter –β with range; it is clear how it decreases with distance (i.e. the spatial correlation of the errors is higher at farther ranges). This trend might be due to the beam broadening with distance (smoothing of the precipitation field).

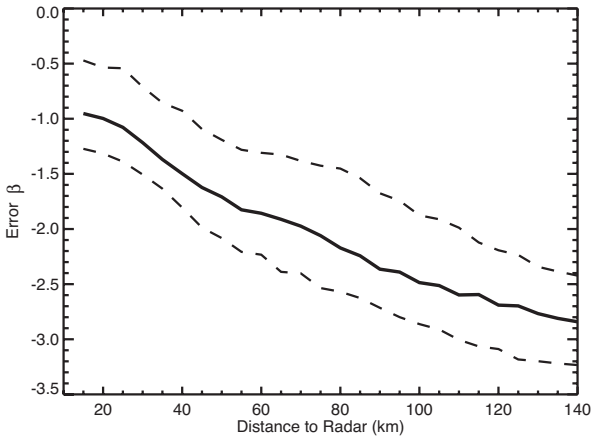

Fig. 6. Evolution of the parameter –β with range. Solid line corresponds to the median of the 291 fields, and dashed lines to the 25 and 75 percentiles.

If we look to the accumulated fields (accumulation of the 291 images), we obtain similar trends for the error fields standard deviation and for the –β parameter (not shown). Fig. 8 shows the accumulations for the reference field and for the simulated fields at three distances (20, 100 and 135 km), and the corresponding error fields. The error field at 20 km shows how the radar overestimates the reference in almost all the domain. In the 100 km error field, we can see that, although the bias is more or less the same that at 20 km (approx. 3 mm; see Fig. 7), the standard deviation of the error field increased and now there is an area where the radar underestimates. The 135 km error field shows that the radar is underestimating in the whole domain except in small areas where it overestimates, increasing the standard deviation of the error field.

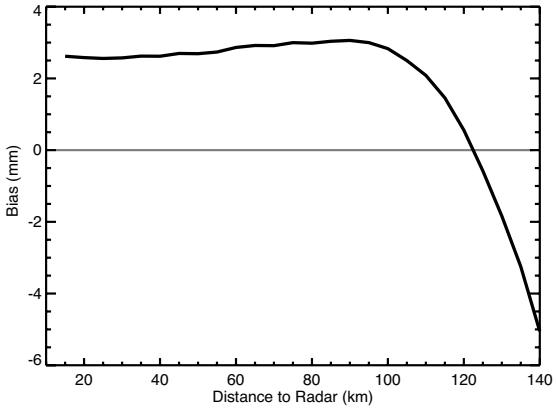

Fig. 7. Bias of the accumulated fields as function of range.

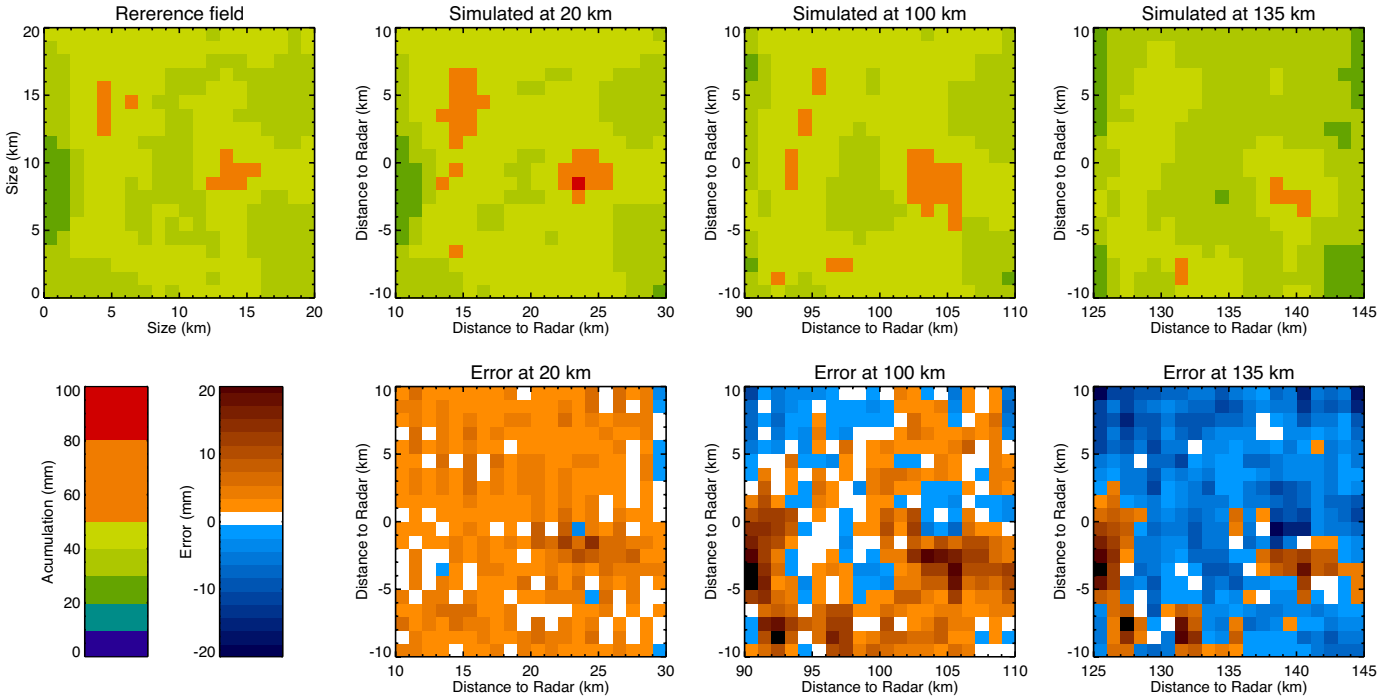

Fig. 8. Accumulated fields for the reference and the simulations at 20, 100 and 135 km (first row), and the corresponding error fields (second row).

5 Conclusions

The presented results show the potential of this simulation approach to study the different errors affecting radar rainfall estimates.

In this first step, we characterized and quantified the errors due to the distance. Using this information, ensembles of radar estimates taking into account the distance error could be produced by adding noise with the appropriate structure to the observations.

Future work will be carried out to extent this preliminary study to various errors (studied each one independently).

Acknowledgements: This work has been carried out in the framework of the EU project FLOODSITE (GOCE-CT-2004-505420). Thanks are due to the Spanish Institute of Meteorology (INM) for providing the radar data.

References

Bellon, A., G. Lee, and I. Zawadzki, 2005: Error statistics of VPR corrections in stratiform precipitation. *J. Appl, Meteor*. **44**, 998-1015.

Doviak, R. J., and D. S. Zrnic, 1992: Doppler radar and weather observations. Academic Press, 562 pp.

Germann, U., M. Berenguer, D. Sempere-Torres, and G. Salvadè, 2006: Ensemble radar precipitation estimation - a new topic on the radar horizon. *ERAD publication series,* **3** (this Volume).

Lee, G. W., A. Seed, I. Zawadzki, 2005: Precipitation physics: the structure of precipitation and its modeling in space and time. *Preprints, 32nd Int. Conf. on Radar Meteorology*, Albuquerque, EUA, Amer. Meteor. Soc. CD.

Llort, X., M. Berenguer, M. Franco, R. Sánchez-Diezma, and D. Sempere-Torres, 2006: 3D downscaling model for radar-based precipitation fields. *Meteorol. Z.* (in press).